Undulator schemes with the focusing properties for the VUV-FEL at the TESLA Test Facility

J. Pflüger and Yu.M.Nikitina*
Hamburger Synchrotronstrahlungslabor HASYLAB
at Deutsches Elektronen-Synchrotron DESY
Notkestr. 85, 22603 Hamburg, Germany
*) *Permanent address: Department of Mathematical Physics,*
Tomsk Polytechnical University , 634004 Tomsk, Russia

February 5, 1996

Abstract

At DESY in Hamburg a Free Electron Laser for the VUV spectral range at 6.4 nm using Self Amplified Spontaneous Emission is under construction. It will use the electron beam of the TESLA Test Facility. One of the main components is an undulator of 30 m length. In order to keep the electron beam-size small over the length of the undulator an alternating quadrupole field has to be superimposed. In this paper five different undulator schemes, which have these properties are studied using the 3D code MAFIA. The results are compared and discussed.

Introduction

At DESY in Hamburg it has been decided to build a Free Electron Laser in the VUV spectral range (VUV-FEL) based on the principle of Self Amplified Spontaneous Emission (SASE) [1]. It will make use of the electron beam of the TESLA Test Facility (TTF), which will provide a very low normalized emittance ($\leq 2\pi mm \cdot mrad$), an ultra short bunch length ($50\mu m$) and peak currents of about 2500 A [2]. These properties will make the TTF an excellent driver for an FEL. At a nominal energy of 1 GeV it will operate at a wavelength of 6.4 nm. In contrast to FEL's using optical cavities a SASE FEL needs a very long undulator of a total length of about $30m$. Furthermore the undulator needs a superimposed quadrupolar field with an alternating gradient to produce a FODO lattice, which is used to keep the beam size small over the whole undulator length.

This paper deals with five different magnetic layouts based on permanent magnet (PM) technology to produce an undulator field plus a superimposed

quadrupolar field. Two of these layouts were already published [3, 4, 5, 6]. The remaining three are new proposals.

A detailed study and comparison of these structures using the 3-D code MAFIA is presented. Only strong focusing as caused by quadrupolar fields is considered. Natural focusing as is present in any periodic field is neglected [7]. The study is not a final design study for the undulator for the VUV-FEL. Its intention is to find out the best way of designing an undulator with the required properties. However, undulator parameters which allow for the required optical properties were chosen.

Choice of the undulator parameters

The parameters of the undulator which determine the optical properties were chosen on the basis of the following considerations:

1. The energy of the 1st harmonic should be 192 eV corresponding to 6.4 nm at an electron energy 1 GeV.
2. The K-parameter has to be larger than unity in order to keep the saturation length in an acceptable limit.

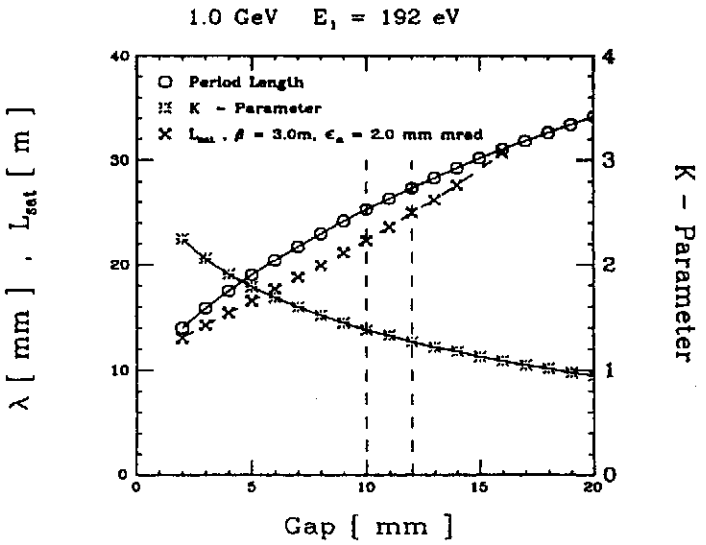

Figure 1: *Dependence of the period length, the K-parameter and the saturation length on the design gap. The constraint is to keep the first harmonic fixed at 192 eV. The dashed vertical line indicates the region of interest for the VUV-FEL at the TTF.*

Table 1 Summary of undulator parameters		
Design gap	12 mm	10 mm
Period length	27.3 mm	25.27 mm
Peak field	0.5 T	0.584 T
K-parameter	1.27	1.38
Radiation characteristics at 1.0 GeV		
γ	1956	1956
Radiation wavelength	6.42 nm	6.42 nm
Energy of the 1st harmonic	192 eV	192 eV
Saturation length, $\beta = 3.0\ m$	24.96 m	22.3 m
Saturation power, $\beta = 3.0\ m$	1.49 GW	1.622 GW

Hybrid PM technology [8] is used to produce the periodic field. For NdFeB magnet material a maximum field of

$$B_{max}[T] = 3.44\, exp\left\{-5.08\frac{g}{\lambda} + 1.54\left(\frac{g}{\lambda}\right)^2\right\}$$

can be assumed (g is the undulator gap, λ is the period length). The relationship is valid for $0.07 < g/\lambda < 0.7$.

Fig.1 shows the influence of the design gap onto the choice of the period length under the restriction given by conditions 1. and 2. Fig.1 also shows the effect of a smaller design gap on the K-value. Using the formulae of Kim and Xie [9] the effect on the saturation length is calculated assuming an average β-function of 3.0 meter and the normalized design emittance of $2\pi\ mm \cdot mrad$. Generally, the lower the design gap, the shorter the design period length.

To be on the conservative side a magnetic design gap of 12 mm is chosen. This value keeps resistive wall wake field effects in an acceptable limit. Also protection against the radiation damage in the magnetic structure caused by missteered or deflected electrons is better if the design gap is larger. However, a minimum magnetic gap of 10 mm seems possible if this questions are finally cleared.

In Table 1. the undulator parameters are summarized. The first column shows the values valid for a design gap of 12 mm. The second column shows the results if this value is reduced to 10 mm.

Magnetic fields and gradients

In the iron free region inside the gap, an undulator field with a superimposed quadrupole field can be derived from a scalar potential of the form:

$$\chi = -\frac{B_{max}}{\kappa} \sinh \kappa y \sin \kappa z - Qxy \tag{1}$$

Here B_{max} is the peak field, Q the gradient and $\kappa = 2\pi/\lambda_0$ where λ_0 is the period length. The coordinate system is shown in Fig.2. The magnetic field is obtained by:

$$\vec{B} = -\nabla\chi \tag{2}$$

where ∇ is the gradient operator.

The ideal magnetic field distribution is consequently given by:

$$\begin{aligned} B_x &= Qy \\ B_y &= B_{max} \cosh \kappa y \sin \kappa z + Qx \\ B_z &= B_{max} \sinh \kappa y \cos \kappa z \end{aligned} \tag{3}$$

From (3) the gradient may be obtained by:

$$\frac{\partial B_x}{\partial y} = \frac{\partial B_y}{\partial x} = Q \tag{4}$$

The field distributions, which can be generated by discrete permanent magnet arrays may differ considerably from the ideal ones given by eqs.(3). First, besides the pure quadrupole term Q, higher multipoles, such as octupoles *etc.*, may be present, especially when well away from the symmetry axis. Second, the gradient needs not to be constant along the electron beam direction. However, it will have the periodicity of the period length. It is therefore very useful to distinguish between the local, z-dependent gradient given by $Q = \partial B_y/\partial x$ and a gradient Q_{ave} averaged over an undulator period, which is defined as:

$$Q_{ave}(x,y) = \frac{1}{\lambda_u} \int_z^{z+\lambda_u} \frac{\partial B_y(x,y,z')}{\partial x} dz' = \frac{1}{\lambda_u} \frac{\partial}{\partial x} \int_z^{z+\lambda_u} B_y(x,y,z') dz' \tag{5}$$

where the integral in the second equation is the first field integral.

Undulator schemes with focusing properties

1. Varfolomeev Undulator (VU)

Fig.2 shows a 3D view of a proposal by the group of Varfolomeev from the Kurchatov Institute in Moscow [3, 4]. One and a half periods are shown for numerical reasons. The model consists of a regular hybrid structure and an

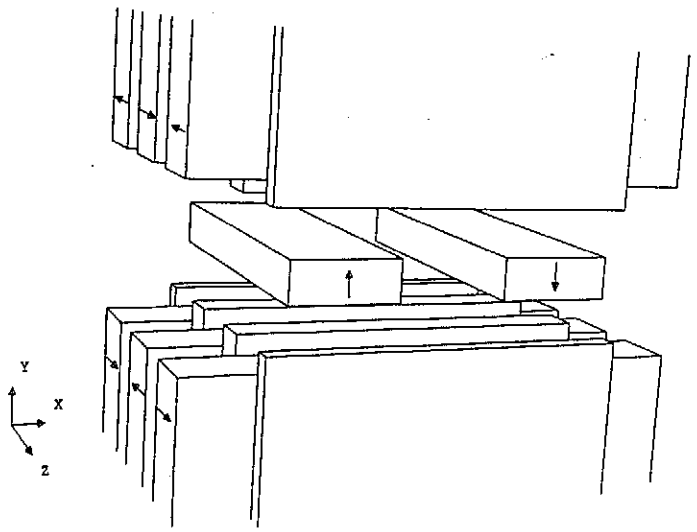

Figure 2: *3-D perspective view of 1 1/2 periods of a hybrid undulator following the proposal of Varfolomeev et al. (see* [3, 4]*).*

additional focusing attachment consisting of two magnets with anti-parallel polarization to provide the focusing.

The undulator period length and the length of the focusing attachment are completely independent from each other. In fact it is possible to convert any regular planar undulator into a focusing one by using these additional side magnets.

The focusing strength can be adjusted by changing the separation distance between the magnets.

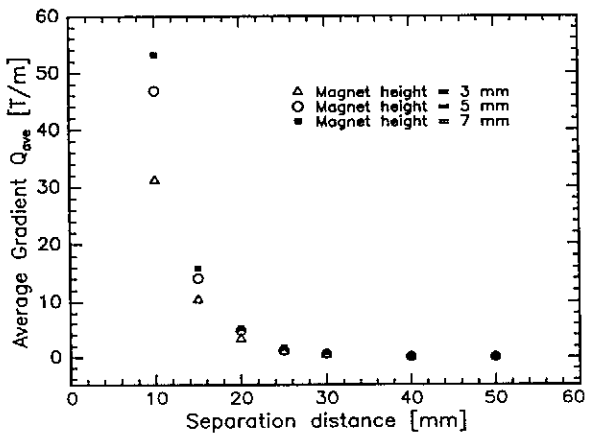

Figure 3: *The dependence of the average gradient on the separation distance and the height of the side magnets.*

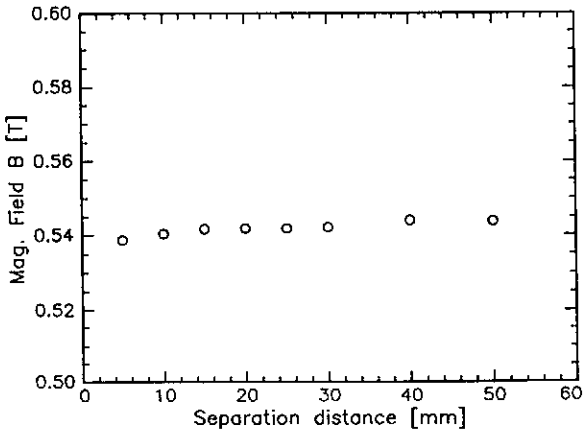

Figure 4: *The dependence of the central peak field on the separation distance between the side magnets.*

The influence of a number of design parameters is studied in Fig.3-6. Fig.3 shows the dependence of the averaged gradient on the separation distance between the magnets for three different magnet heights. It can be seen that the

distance has to be between 10 and 15 mm in order to obtain gradients well above 10 T/m. A minimum separation distance equal to the gap is however needed if a circular beam tube is to be used.

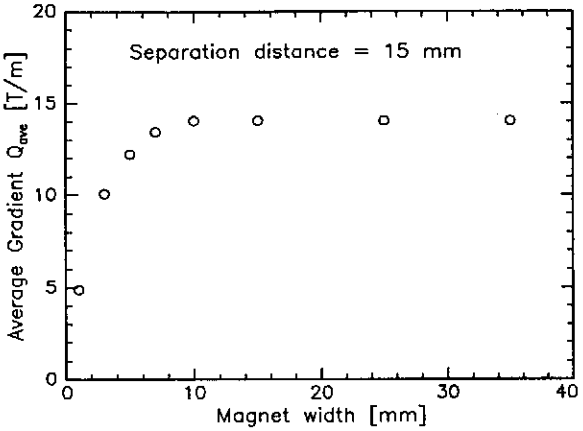

Figure 5: *The dependence of the gradient on the width of side magnets for* $d = 15mm$.

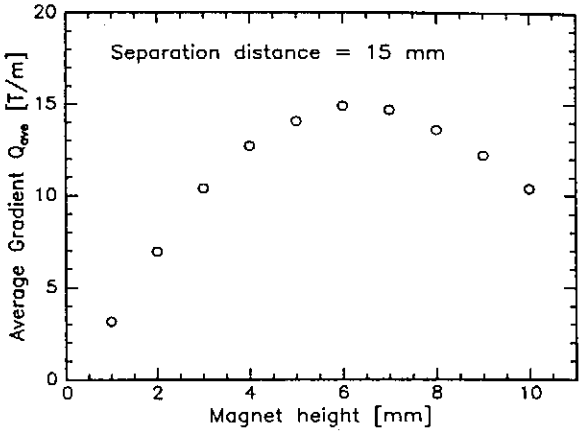

Figure 6: *The dependence of the gradient on the height of the side magnets for* $d = 15mm$.

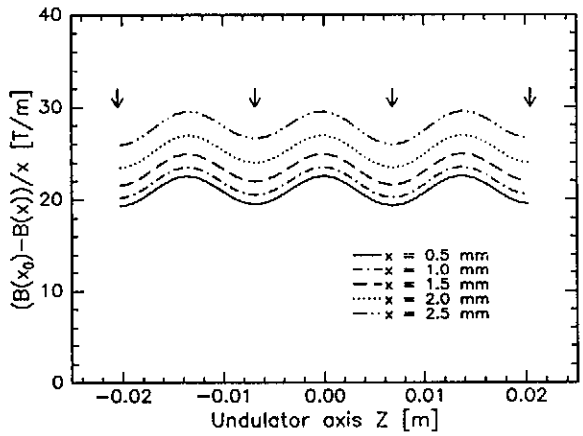

Figure 7: *The profile of the gradient along the* z*-axis for different values of* x*. The location of the poles is indicated by arrows.*

Fig.4 shows that the peak field on axis is independent of the separation distance and therefore of the focusing strength. This is essential for building an alternating gradient structure consisting of sections with positive, zero and negative gradients.

The influence of the magnet width and height is studied in Figs.5 and 6.

Fig.5 clearly shows that for our parameters the average gradient does not increase significantly for a width exceeding 10 mm where it approaches a value of Q_{ave} ~14 T/m. To be on the safe side we chose the width of the side magnets to be equal to 15 mm for the following calculations.

Fig.6 shows the average gradient as a function of the magnet height. There is an optimum at about 7 mm. For small heights a continuous increase is

observed. If the height gets larger the magnets get too close to the pole tips, which then act as a magnetic short circuit and cut off some of the field lines.

Fig.7 shows the variation of the field gradient along the undulator axis.The gradient varies by about 3 T/m which for the cases plotted in Fig.7 is roughly independent of the x displacements.

The field gradient depends on x. This means that higher components (octupoles, dodekapoles *etc.*) are present as well. For the TTF the RMS beam-size is only about 0.05 mm which is ten times smaller than the smallest value plotted in Fig.7. It was chosen this way, in order to obtain sufficient numeric accuracy. The higher order contributions will play only a minor role at these small dimensions.

The variation of the field gradient will induce some additional periodic perturbation of the field for electrons going off axis. For $x = 0.05$ mm this can be estimated to be in the order of $1.5 \cdot 10^{-4}$ T which amounts 0.028% of the peak field. This value is very small as compared to typical field errors to be expected, which are in the range from 0.1 to 0.4%.

Table 2 **Parameters for VU**	
Period length	27.3 mm
Peak field	0.54 T
Pole gap	12 mm
Pole overhang	0.5 mm
Focusing magnet separation	12 mm
Magnet	70×50×8.5 mm
Pole	50×40×5.15 mm
Focusing magnet	15×5×length of quad.
Gradient	~20 T/m

The inherent disadvantage of the VU is that it almost completely circumbuilds the electron beam-pipe. Exact magnetic measurements are therefore very difficult to perform. In addition, the focusing magnets have to be removed at least on one side after the measurement in order to insert the vacuum chamber.

Table 2 shows a set of preliminary parameters which can be used for the VUV-FEL at the TTF. The height of the magnets was chosen to be only 5 mm, so that clearance to the pole tips of 3.5 mm is left. This eventually allows a specially shaped field sensors to be used for the magnetic measurements on the undulator axis.

2. Tilted Pole Undulator (TPU)

Fig.8 shows a second alternative, the tilted pole undulator (TPU). The idea of the TPU is not new and in the past it was used on several undulators for FEL's. Ref.[5] might serve as an example. Ref.[6] is a more recent proposal for the LCLS at Stanford.

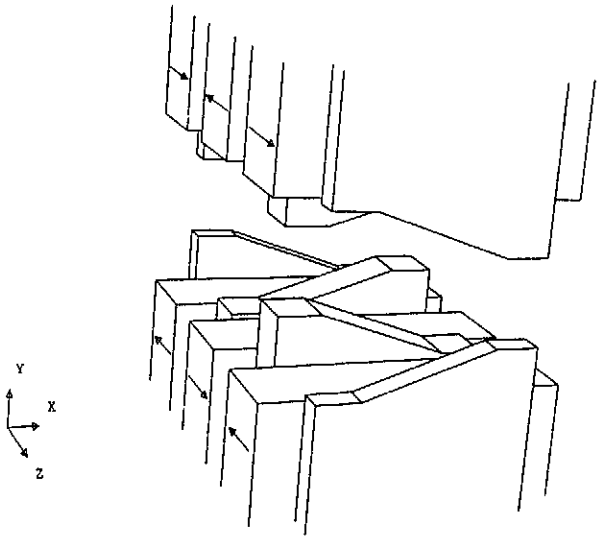

Figure 8: *The 3-D view of 1 1/2 periods of Tilted Poles Undulator (TPU).*

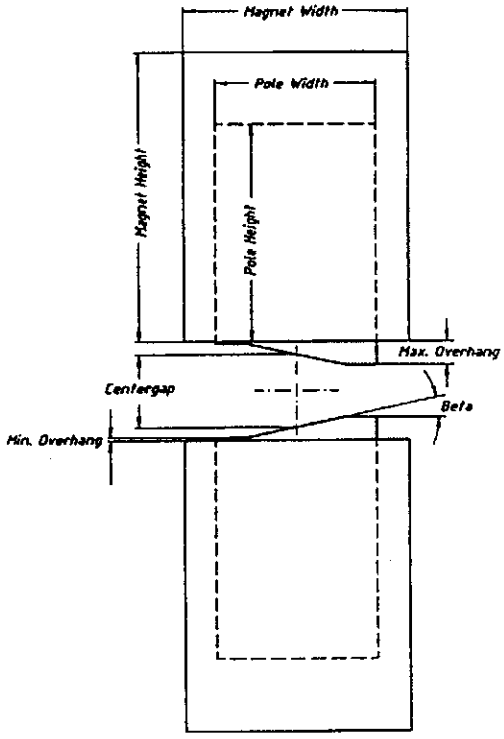

Figure 9: *Front view of the TPU giving the definitions of the design parameters shown in Table 3. Beta is the tilt angle.*

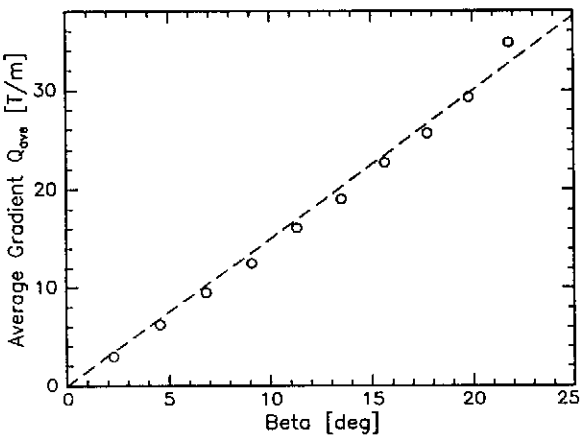

Figure 10: *The dependence of the gradient on the tilt angle. The dashed line shows the results using the scalar potential formalism of* [10].

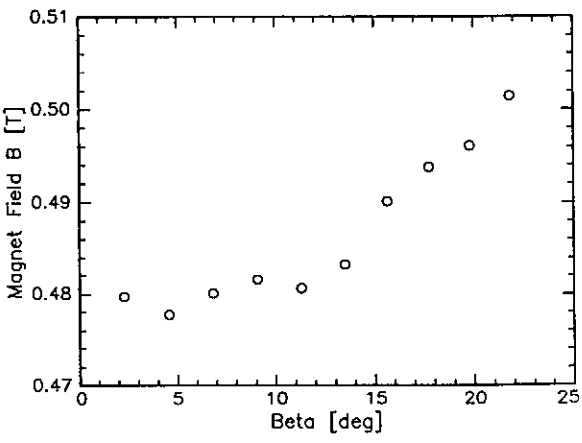

Figure 11: *The dependence of the central peak field on the tilt angle.*

The gap shown in this 3D view is opened beyond scale to provide a better spatial impression. The poles are tilted in alternating directions near the beam

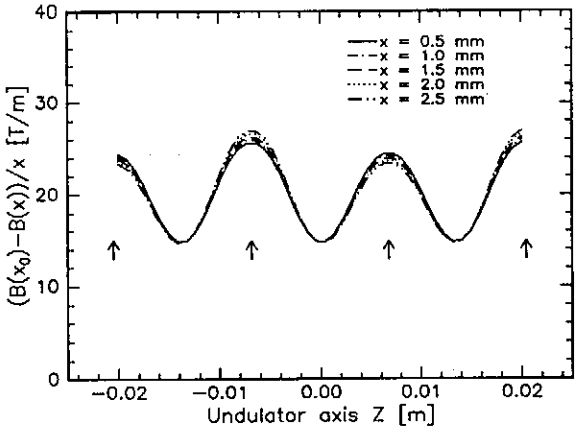

Figure 12: *The dependence of the gradient along the z-axis for different x-values. The arrows indicate the location of the canted poles.*

Table 3 Parameters for TPU	
Period length	27.3 *mm*
Peak field	0.5 T
Center pole gap	12 *mm*
Tilt angle (Beta)	~15 *deg*
Min. pole overhang	0.5 *mm*
Max. pole overhang	4.5 *mm*
Magnet	35×50×8.5 *mm*
Pole (center)	25×40×5.15 *mm*
Gradient	~20 T/m

axis and flattened for larger x-values to avoid strong saturation in the case when the pole ends are situated too close to each other. This negative effect is especially strong for higher values of the gradient. Fig.9 shows a cross-sectional view along the undulator axis and gives a definition of the design parameters shown in Table 3.

It can be shown that tilted pole faces give a good approximation to a scalar potential of the form given by eq.(1) [6, 10]. In the vicinity of the z-axis, the field given by the pole arrangement shown in Fig.8 is very close to the expected behavior.

Fig.10 shows the averaged gradient as a function of the tilt angle. The curve is almost linear. The dashed line shows the gradient calculated using the slope of the equipotential surfaces. This analytic method is described in more detail in [10]. The agreement is very good. One sees that at a tilt angle of about 15^0,

a gradient of 20 T/m can easily be reached. In principle even higher gradients exceeding 30 T/m are possible.

However, Fig.11 gives an upper limit for reasonable gradients of a quadrupole field. The undulator peak field as a function of the tilt angle is shown. It is seen that, up to about 15^0, there is only a minor effect on the peak field. Above 15^0 the peak field changes. For a TPU consisting of sections with positive, zero and negative gradients, the tilt angle should therefore stay below 15^0 since this makes the transitions between sections of different gradients simple and further adjustment may not be needed. Table 3 shows design values for the TPU which might be used for the TESLA-FEL. The magnetic width is considerably smaller than in the case of the VU allowing comparatively large tilt angles of the poles.

Fig.12 shows the variation of the gradient along the undulator axis. In contrast to the VU its maximum values are under the canted pole pieces. Note, however, that there are slightly different values for positive and negative poles. In addition, the gradient is almost constant over the full $+/-2.5$ mm horizontal range. Thus the content of higher harmonics is low. The amplitude at 0.05 mm of the variation amounts to $5.5 \cdot 10^{-4}$ T which is about 0.11% of the field amplitude. This is still smaller than the external errors due to magnetic imperfections.

3. Staggered Pole Undulator (SPU)

Fig.13 and 14 show a third alternative to be investigated for a focusing structure.

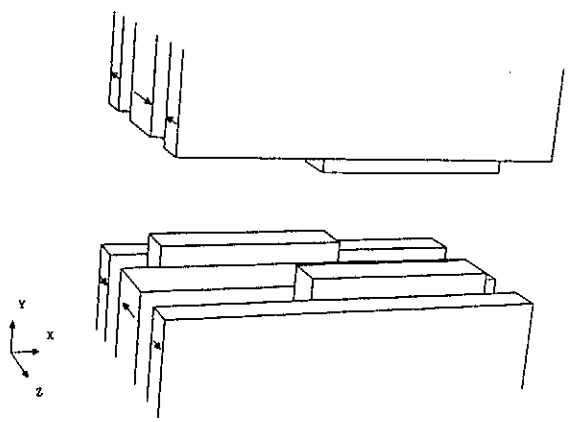

Figure 13: *The 3-D view of one period of SPU1 model of a hybrid undulator.*

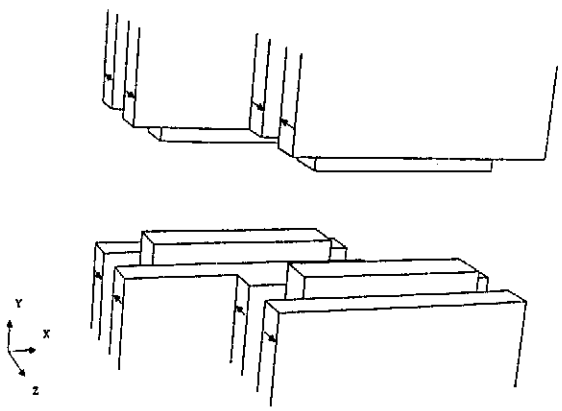

Figure 14: *The 3-D view of one period of SPU2 model of a hybrid undulator.*

The "staggered pole undulator" (SPU) is shown in a perspective view in two configurations in Fig.13 and 14. First, the basic principle is demonstrated in Fig.15. In a SPU the poles are "staggered" alternatively to the right and to the left.

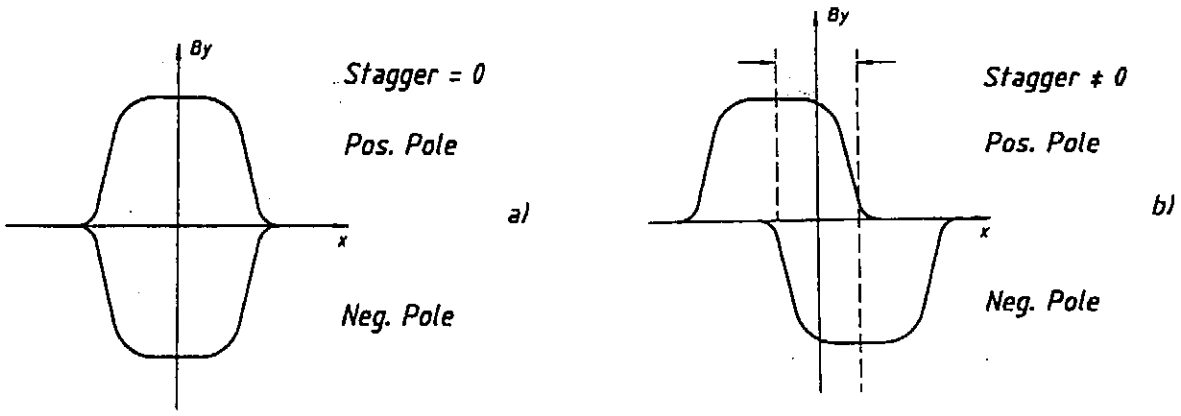

Figure 15: *Working principle of the SPU.*

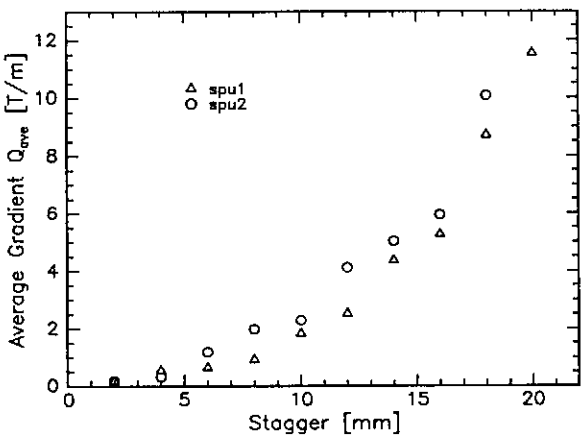

Figure 16: *The dependence of the gradient on the shift Δx of the poles.*

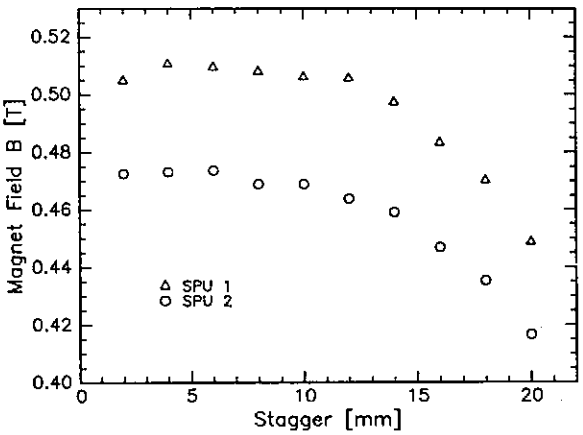

Figure 17: *The dependence of the peak field in gap on the shift of the poles.*

Fig.15a demonstrates the situation in a normal undulator where the poles are not staggered. The field profile of B_y along x is symmetric for positive and negative poles. If, however, the stagger is non-zero, a situation as shown in Fig.15b can be found. In this example, positive poles are shifted to the left and negative ones to the right. Only electrons at $x = 0$ will suffer no deflection. At negative x-values, there is now an excess of positive field and at positive x-values the opposite is true. In this way an approximately quadrupolar field near $x = 0$ is generated. In order to obtain an appreciable field difference the stagger has to be of the order of at least half of the pole width.

In the SPU1 model shown in Fig.13 the magnets are chosen very wide so that the overhang of the magnets is larger than the stagger. In the SPU2 model shown in Fig.14 the halves of magnet blocks are staggered as well. Fig.16 shows the gradient for the two SPU's as a function of the stagger. The gradient is very low up to about 12 to 15 mm. At 20 mm, about 15 T/m can be reached. In contrast Fig.17 shows the peak field as a function of the stagger. It differs by a few percent for the two types due to the different volumes of the main magnets

Table 4 Parameters for SPU		
	SPU 1.	SPU 2.
Period length	27.3 mm	27.3 mm
Peak field	0.45 T	0.42 T
Pole gap	12 mm	12 mm
Pole overhang	2.5 mm	2.5 mm
Magnet	50×50×8.5 mm	35×50×4.25 mm
Pole	25×40×5.15 mm	25×40×5.15 mm
Stagger	20 mm	20 mm
Gradient	~11.5 T/m	~13.5 T/m

and is approximately constant to about 10 to 12 mm. In the region of higher gradients, the peak field decreases by more than 10%. This decrease, however, makes the SPU not a good candidate for alternating gradient structures, so that we refrain from further investigations.

4. Four Magnet Focusing Undulator (4MFU)

Fig.18 shows another planar proposal using four additional magnets per half-period.

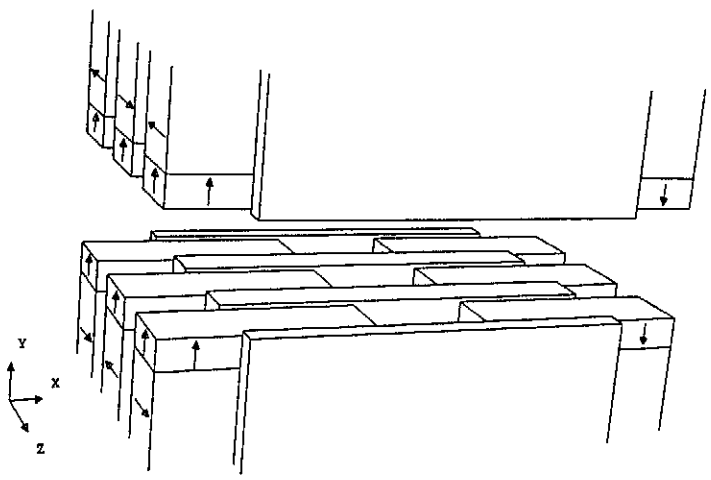

Figure 18: *3-D perspective view of 1 1/2 periods of the 4MFU hybrid undulator.*

The magnets providing the undulator field (magnetized along z) have been recessed by 6 mm so that there is now space for the focusing magnets, which are

polarized parallel or anti-parallel along y, as can be seen in Fig.18. This configuration is a modified adoption of Tatchyn's proposal for generating quadrupolar fields with PM arrays [11]. The gap in this configuration is completely free.

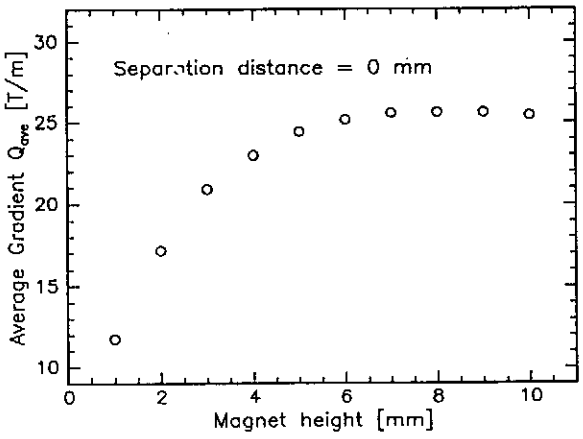

Figure 19: *The dependence of the gradient on the height of the focusing magnets.*

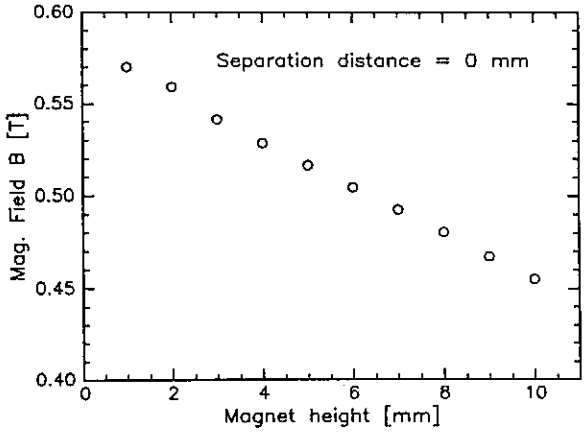

Figure 20: *The dependence of the peak field in gap on the height of the focusing magnets.*

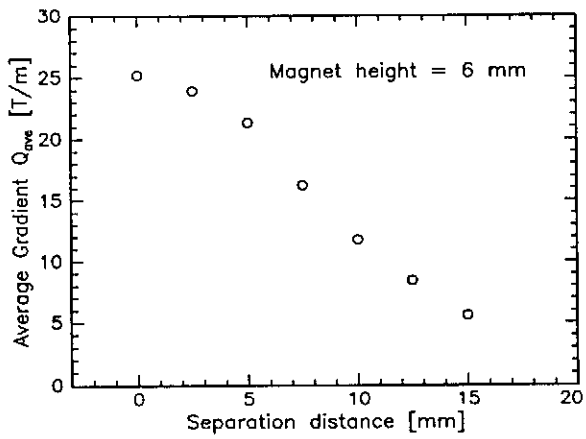

Figure 21: *The dependence of the gradient on the separation distance between the focusing magnets.*

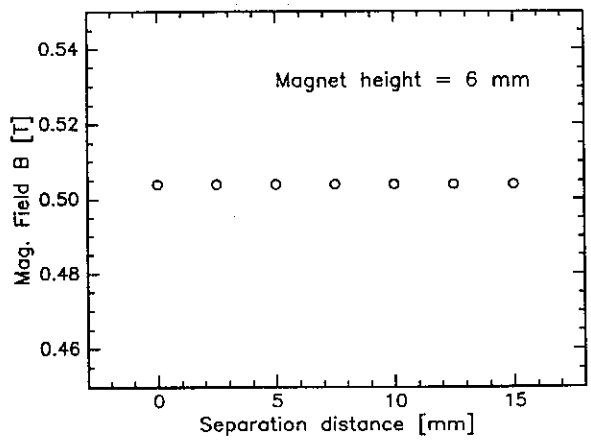

Figure 22: *The dependence of the peak field in gap on the separation distance.*

Fig.19 shows the influence of the height of the focusing magnets onto the average gradient, Fig.20 shows this influence onto the peak field. It is understandable that the peak field increases with decreasing height of the focusing magnets while the gradient increases. The separation distance between the magnets in these calculations was taken to be zero.

Fig.21 shows the influence of the separation distance on the average gradient and Fig.22 its influence onto the peak field. An average gradient up to about 25 T/m can be obtained in this way. Fig.22 demonstrates that the value of peak field in the gap is not affected at all by changing the separation distance in very much the same way as in the case of the VU undulator.

Table 5 summarizes the characteristic dimensions for this model. It is seen

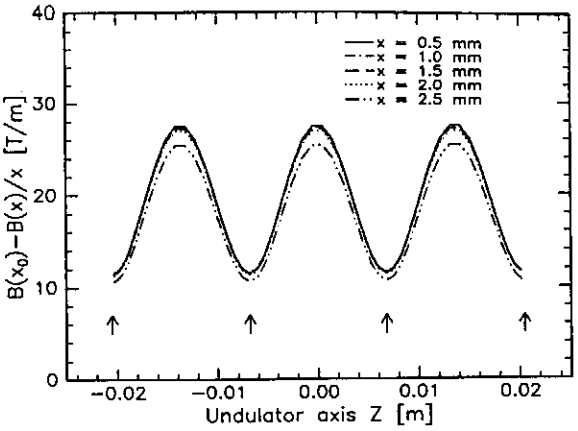

Figure 23: *The variation of the gradient along the undulator axis for different x values. Pole locations are indicated by arrows.*

Table 5 Parameters for 4MFU	
Period length	27.3 mm
Peak field	0.5 T
Pole gap	12 mm
Pole overhang	0.5 mm
Focusing magnet separation	5.5 mm
Magnet	70×50×10 mm
Pole	50×40×3.65 mm
Focusing magnet	15×6×10 mm
Gradient	20 T/m

that the magnet length was slightly enlarged to 10 mm and the pole length reduced correspondingly when compared with the previous examples.

Fig.23 shows the variation of the field gradient along the z-axis. Its amplitude at 0.05 mm is estimated to be $8.4 \cdot 10^{-4}$ T which is 0.17% of the peak field. As can be seen in Fig.23 the gradient is almost constant over the full $+/-2.5$ mm range.

5. The Side Magnets Focusing Undulator (SMFU)

Fig.24 shows the fifth alternative using four additional side magnets which may be extended over several poles (SMFU).

The four focusing magnets are closely brought to the beam by choosing the width of the poles as small as possible. Only 10 mm were chosen for the pole width. The focusing magnets are embedded in the main magnets producing

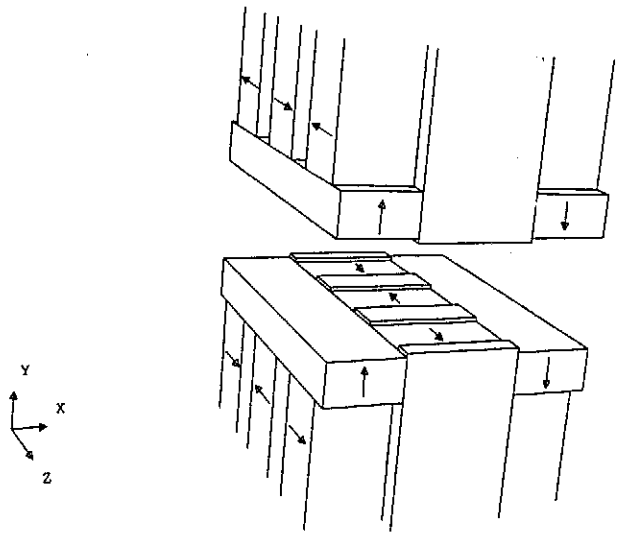

Figure 24: *3-D perspective view of 1 1/2 periods of a SMFU hybrid undulator.*

the undulator field. In very much the same way as in the case of the previous structures Figs.25-28 show the influence of some important design parameters.

Figs.25 and 26 show the average gradient and the peak field as a function of the height of the side magnets. The situation is analogous to the 4MFU case. At a moderate loss of peak field in the gap a field in excess of 0.5 T and a gradient larger than 22 T/m can be reached.

Figs.27 and 28 demonstrate the tunability of the side magnets as a function of the separation distance. The minimum distance of 10 mm is given by the pole width which was chosen to be considerably smaller than in the previous structures. The peak field stays constant as a function of the magnet separation.

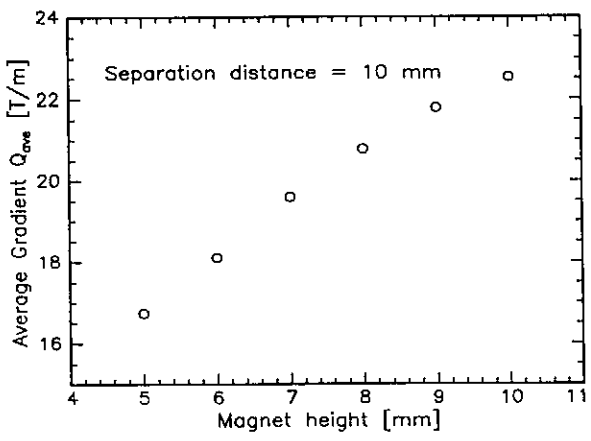

Figure 25: *The dependence of the gradient on the height of side magnets.*

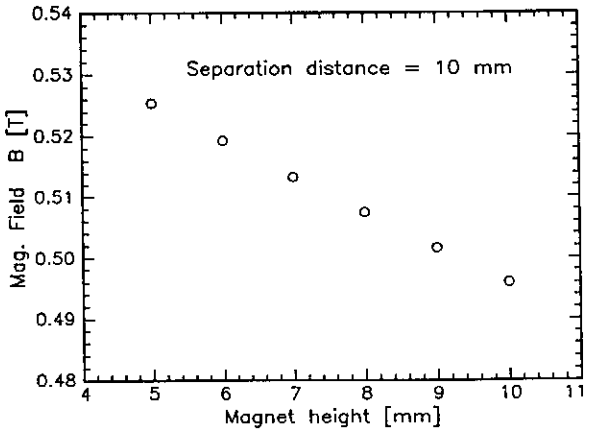

Figure 26: *The dependence of the peak field in gap on the height of the side magnets.*

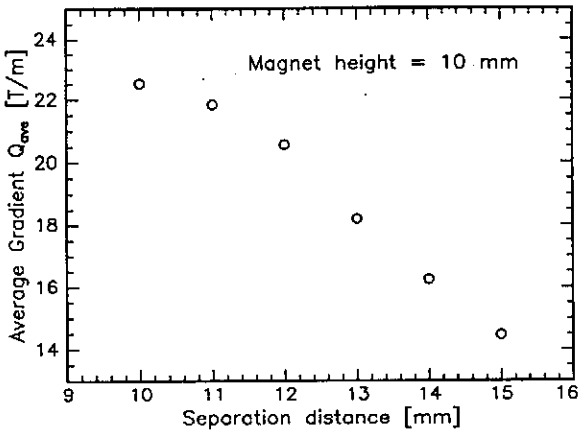

Figure 27: *The dependence of the gradient on the separation distance between the side magnets.*

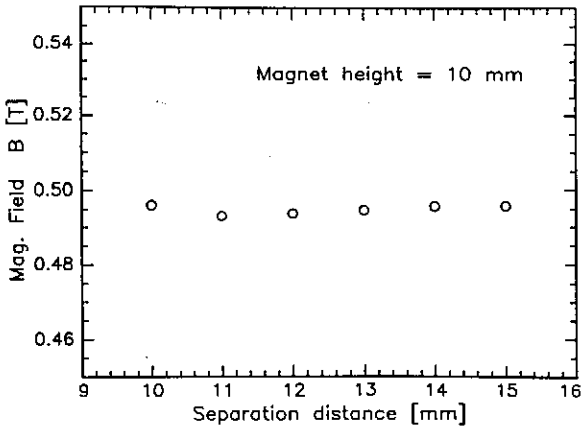

Figure 28: *The dependence of the peak field on the separation distance between the side magnets.*

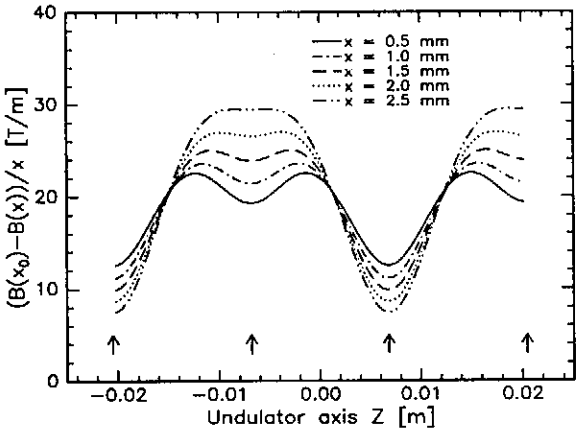

Figure 29: *The variation of the gradient along the z-axis for different values of x. Arrows indicate the locations of the poles.*

This fact is again analogous to the VU and 4MFU cases.

Finally, Fig.29 shows as in the previous cases the variation of the field gradient along z. It's shapes and amplitudes are strongly x-dependent. However, taking the gradient variation for x =0.05 mm an amplitude of $5.4 \cdot 10^{-4}$ T is estimated corresponding again to a 0.11% field error. Table 6 summarizes the preliminary design parameters for the SMFU.

Table 6 Parameters for SMFU	
Period length	27.3 mm
Peak field	0.5 T
Pole gap	12 mm
Pole overhang	0.5 mm
Focusing magnet separation	12.5 mm
Magnet	40×50×10 mm
Pole	10×40×3.65 mm
Focusing magnet	15×10×length of quad.
Gradient	~20 T/m

Summary

Five different PM based structures which can be build to include quadrupole focusing have been described in detail in the previous sections. To compare the properties of these structures and to find out the best type for the 30 m long VUV-FEL at the TESLA Test Facility four criteria should be considered:

1. Accessibility of the field region.

   The requirements on the quality of the magnetic structure will be high. It is anticipated that the tolerable field error level will be very small and must not exceed 0.2-0.4% RMS at most, which is at the limit of technical feasibility. Also the focusing properties will have to be well defined. Therefore precise magnetic measurements and subsequent tuning and/or shimming techniques will be an essential part to obtain these low tolerances. High precision magnetic measurements need access to the field region, which will be later occupied by the electron beam.

   For the insertion of the vacuum chambers after the final measurements a planar gap is of great advantage. Otherwise a part of the magnetic structure needs to be disassembled for this purpose. It is however not sure that the magnetic properties are exactly identical after this reassembly than they were before. There might be small displacements and misalignments or hysteretic effects may play some role. In any case, disassembling and subsequent reassembling induce some potential sources of errors, which cannot be detected and controlled. Therefore purely planar structures should be prefered. Clearly the VU and TPU are no good candidates on the basis of these arguments.

2. Peak field dependence on focusing strength.

   It is important that the peak field level is independent of the gradient. An alternating gradient structure can only be realized if this condition is fulfilled. The SPU does not satisfy this requirements and therefore drops out completely.

3. Fine tuning of the field gradient.

   Fine tuning of the field gradient is highly recommended. In this way the axis of the superimposed quadrupolar field can be exactly centered and the individual sections can be made identical.

   The VU, 4MFU and SMFU offer this possibility. In all this cases it is sufficient that the separation distance between the focusing magnets is adjustable.

4. Variation of the field gradient along z.

   In all structures proposed so far the field gradient along the electron beam is not constant. Since the RMS beam-size is about 0.05 mm for the undulator section in the TESLA Test Facility this will induce some additional field variations. Table 7 shows a summary of characteristics for all structures investigated. The Staggered Pole Undulator has not been included because it is not a good candidate for the reasons mentioned above. The VU offers the lowest perturbation amplitude. The relative contribution is only 0.028% . TPU and SMFU are about the same but at an almost four times increased level, while the 4MFU shows even higher contribution. Preliminary results indicate that the influence of these periodic perturbations onto FEL performance is rather small. This will be subject to another publication [12].

To summarize the arguments of this discussion it turns out that only the "Four Magnet Focusing Undulator" (4MFU) and the "Side Magnet Focusing Undulator" (SMFU) are good candidates, which provide enough focusing strength. There exist some possibility for fine tuning of the focusing strength. Furthermore, the peak field amplitude is independent of quadrupole strength.

Acknowledgment

One of the authors (Y.M.N.) would like to thank HASYLAB for the hospitality during her stay in Hamburg and the DAAD for the financial support of this work.

Table 7				
Overview of characteristics of gradient variation				
Undulator type	Var. of gradient @ 0.05 $[T/m]$	Ampl. of variation @ 0.05 $[T]$	B_{max} $[T]$	$\Delta B_{max}/B_{max}$
VU	3.0	1.5×10^{-4}	0.54	2.8×10^{-4}
TPU	11.	5.5×10^{-4}	0.5	1.1×10^{-4}
4MFU	16.7	8.4×10^{-4}	0.5	1.68×10^{-4}
SMFU	10.7	5.4×10^{-4}	0.5	1.1×10^{-4}

References

[1] "A VUV Free Electron Laser at the TESLA Test Facility at DESY. Conceptual Design Report", DESY, Hamburg, April, 1995

[2] "TESLA Test Facility Linac - Design report", DESY, Hamburg, March, 1995

[3] A.A. Varfolomeev, A.H. Hairetdinov Nucl.Instr. and Meth. A 341 (1994) 462

[4] A.A. Varfolomeev, V.V. Gubankov, A.H. Heiretdinov, S.N.Ivanchenkov, A.S.Khlebnikov, N.S.Osmanov, S.V.Tolmachev in: Proceedings of the 16th FEL Conference August 21-26, 1994, Stanford, USA

[5] K.E. Robinson, D.C. Quimby, J.M. Slater, IEEE Journal of Quantum Electronics Vol. QE-23, 9 (1987) 1497
D.C. Quimby, S.C. Gottschalk, F.E. James, K.E. Robinson, J.M. Slater, A.S. Valla, Nucl.Instr. and Meth. A 285 (1989) 281

[6] R. Schlüter in: Proceedings of the 16th FEL Conference August 21-26, 1994, Stanford, USA

[7] E.T. Scharlemann, J. Appl. Phys. Vol.48 (1985) 2154-2161

[8] K. Halbach, Journal de Physique, C1, suppl.2, (1983) C1-211

[9] K.J. Kim, M.Xie Nucl.Instr. and Meth. A 331 (1993) 359

[10] "The Art and Science of Magnet Design", Vol. 2, p.19 ff., Workshop on Magnet Design, February 1995, Berkeley, USA

[11] R.Tatchyn, Nucl.Instr. and Meth., A 341 (1994) 449

[12] Yu.M.Nikitina, J.Pflüger, E.Schneidmiller, in preparation